The Medial Temporal Lobe Structure and Function Support Positive Affect

Weipeng Jin
Tianjin Huanhu Hospital
Jie Feng
Tianjin Normal University
Wenwei Zhu
Tianjin Normal University
Bin Zhang
Tianjin Normal University
Shuning Chen
Tianjin Normal University
Shiyu Wei
Tianjin Normal University
Pinchun Wang
Tianjin Normal University
Kun Deng
Tianjin Normal University
Yajie Wang
Tianjin Normal University
Manman Zhang
Tianjin Normal University
Shaofeng Yang
Tianjin Normal University
Hohjin Im
University of California Irvine
QIANG WANG (✉ wangqiang113@gmail.com)
Tianjin Normal University https://orcid.org/0000-0002-1081-6690

Research Article

Keywords: positive affect, multivariate pattern analysis, VBM, hippocampus, perirhinal cortex

Posted Date: March 18th, 2022

DOI: https://doi.org/10.21203/rs.3.rs-1389084/v1

Abstract

Positive affect (PA) is not only associated with individuals' psychological and physical health, but also their cognitive processes. However, whether medial temporal lobe (MTL) and its subfields' volume/functional connectivity can explain individual variability in PA remains understudied. We investigated the morphological (i.e., gray matter volume; GMV) and functional characteristics (i.e., resting-state functional connectivity; rsFC) of PA combined with univariate and multivariate pattern analyses (MVPA) using a large sample of participants (n = 321). We simultaneously collected the T1-weighted (n = 321), high-resolution MTL T2-weighted, and resting-state functional imaging data (n = 209). The MTL and its subfields' volumes, including the CA1, CA2 + 3, DG, and subiculum (SUB), perirhinal cortex (PRC), and parahippcampus (PHC), were extracted by automatic segmentation of hippocampal subfields (ASHS) software. The morphological results revealed that GMVs in the prefrontal-occipital and limbic (i.e., hippocampus, amygdala, and PHC) systems were associated with variability in PA at the whole-brain level using MVPA but not univariate analysis. Linear regression results further revealed a positive association between the MTL subfields' GMV, especially for the right PRC, and PA after controlling for several covariates. PRC-seed-based rsFC analyses further revealed that its couplings with the fronto-parietal-occipital system predicted PA in both univariate and MVPA. These findings provide novel insights into the neuroanatomical and functional substrates underlying human PA trait. Findings also suggest critical contributions of the MTL and its subfield of the perirhinal cortex, but not hippocampal subfields, as well as its functional coupling with the fronto-parietal control-system on the formation of PA.

Introduction

Positive Affect (PA) typically refers to feelings that correspond to pleasurable or hedonic interactions with one's environment, such as happiness and excitement (Clark et al., 1989). Such feelings are stable and long-lasting, thereby distinguishing the construct from moods and emotions while still sharing common characteristics (Russell & Carroll, 1999). PA is not only associated with psychological and physical health (Perkinsporras et al., 2008; Pressman & Cohen, 2005), but also influences cognitive processes, such as working memory (Yang et al., 2013), decision-making (Isen, 1993), attention selection (Rowe et al., 2007), and problem solving (Isen et al., 1987). Higher levels of PA yield a number of cognitive, interpersonal, physiological, and subjective well-being benefits that promote resilience against adverse situations (Diamond & Aspinwall, 2003; Lyubomirsky et al., 2005). In contrast, lower levels of PA are often accompanied by increased risk for several psychiatric disorders, including problematic substance use (Martinotti et al., 2012), depression/anxiety (Headey, 1993), and externalizing problems (Lunkenheimer et al., 2011). Accordingly, targeting the PA system has been thought to be a promising intervention for treating anxiety and depression (Taylor et al., 2017). Hence, compared to Negative Affect (NA), PA has been gaining attention among scholars, particularly within the field of neuroscience.

The medial temporal lobe (MTL) is a complex brain structure and consists of the hippocampal region (CA fields, dentate gyrus, and subicular complex) and the adjacent perihinal, entorhinal, and parahippocampal cortices (Squire et al., 2004). These adjacent cortices' distinct subfields are thought to be functionally

dissociated, with the hippocampus subserving the recollection memory, the perirhinal cortex supporting recognition and associative memory (Barense et al., 2002), and the parahippocampus contributing to human spatial navigation (Epstein, 2008). Beyond learning and memory, these subfields were also involved in stress regulation and emotional reactivity, including PA (Admon et al., 2009; Pellman & Kim, 2016). When individuals experience external or internal stress, the hippocampus is believed to provide a negative feedback mechanism primarily via the hypothalamic pituitary adrenocortical axis (HPA) (Frodl & O'Keane, 2013). Additionally, patients with parahippocampal cortex lesions have previously exhibited highly abnormal judgments to dissonant music, appraising it as being slightly pleasant in contrast to controls who found it unpleasant (Gosselin et al., 2006). These processes of learning/memory, stress responses, and emotional reactivity/judgment are considered crucial components for PA formation, implicating the hippocampal neural substrates underlying PA.

Longitudinal evidence suggests that the degree of volume reduction in the hippocampus and striatum from early to mid-adolescence can be uniquely predicted by depression beyond time (Whittle, Lichter, et al., 2014; Whittle, Simmons, et al., 2014). Further, roaming entropy (i.e., variability of an individual's physical location to determine experiential diversity) has been demonstrated to promote PA via functional coupling of the hippocampus and striatum (Heller et al., 2020). Hence, we further explored whether such associations between grey matter volume (GMV) in the hippocampus, including its subfields, and PA likewise occur in a large sample of young adults.

Along the longitudinal axis, the hippocampus can be functionally divided into the dorsal, intermediate, and ventral portions (Fenton, 2010). Along the transverse axis, it can also be parcellated as the CA1, CA2, CA3, and dentate gyrus (DG) (Vos et al., 2018; Winterburn et al., 2013). A large body of studies has demonstrated separated functions of these subdivisions on cognition and affect (Bonnici et al., 2013; Cao et al., 2017). In particular, prior imaging studies have found distinct contributions of the hippocampal subfields on relational memory formation whereby the CA2-3 and DG were active when encoding pairs (i.e., face-name) while the subiculum (SUB) was activated during retrieval (Zeineh et al., 2003). Volume reductions of hippocampal subfields, particularly in CA2/3/4 and the hippocampal tail, have been observed in affective disorders, such as bipolar disorder and major depressive disorder, as well as be associated with the progression of these illnesses (Cao et al., 2017; Macoveanu et al., 2021). Moreover, early childhood experiences (e.g., childhood maltreatment) have been identified as critical factors that influence the functional and structural alterations of hippocampal subfields, such as CA3, DG, and SUB (Choi et al., 2012). The perirhinal cortex is also another hub region engaging in recognition memory (i.e., familiarity) (Brown & Aggleton, 2001), object perception (E. A. Murray & Richmond, 2001), within- and between-associations (Suzuki & Naya, 2014), and associative recall (Suzuki & Naya, 2014). PA depends on several mental processes mentioned before (e.g., relational memory, affective experience, emotional responses, and associative encoding/recall) in addition to early environmental factors, which both reshape the experience of PA and buffer the onset of various psychiatric disorders. However, PA's potential association with MTL subfields, including the hippocampal subfield volumes and functional connectivity, needs further empirical examination.

Beyond the isolated brain region, the human brain is organized into several functional networks that exhibit mutual communication and integration between them. To date, intrinsic functional connectivity has been demonstrated as a critical approach to explore and understand the underlying functional networks and their communication (van den Heuvel & Pol, 2010). Recent studies have shown extensive cortical functional connectivity of the human hippocampal system, including the perirhinal cortex via 7T imaging technique (Ma et al., 2022). Moreover, the perirhinal cortex has been documented to receive inputs from prefrontal cortex and visual “what” stream, and exhibits preferential connectivity with a network involved in visceral processing (S. F. Wang et al., 2016). However, what the specific functions of distinct MTL subfields’ functional connectivity on PA are remain unclear.

In the present study, we systematically explored the potential associations between MTL subfields’ volume/functional connectivity and PA via univariate and multivariate pattern analysis (MVPA) approaches in a large sample of young adults (n = 321). To quantitatively assess the grey matter volumes (GMVs) of MTL subfields, we simultaneously collected subjects’ high-resolution T2-weighted and resting-state functional imaging data (n = 209) and employed automatic segmentation of hippocampal subfields (ASHS) tool to divide MTL into seven subfields, such as the CA1, CA2 + 3, DG, subiculum (SUB), perirhinal cortex (PRC), and parahippocampus (PHC) combined with T1-weighted imaging data. Subjects then provided self-reports of PA to be analyzed. Given the current literature, we hypothesized that there are associations of PA with GMVs and functional connectivity at the whole-brain level and MTL-based level, which exhibit specific characteristics.

Materials And Methods

Subjects

Three hundred twenty-one subjects (108 males; age ranged from 17 to 26 years old; Mean age ± SD = 19.93 ± 1.51) participated in this study and their T1-weighted MRI data were collected. Only 209 of participants further included T2-weighted high-resolution MTL and resting-state functional MRI data (70 males; age ranged from 17 to 26 years old; Mean age ± SD = 20.04 ± 1.79). Twenty-six subjects were further excluded due to excessive head motion (framewise displacement [FD] > 0.5 mm) in the following functional connectivity analysis. All subjects were free from neurological or psychiatric history. Informed written consent was obtained from the subjects before formal study procedures were conducted. This study was approved by the Institutional Review Board of the Faculty of Psychology at Tianjin Normal University (No. XL2020-27), China.

Positive Affect and Negative Affect

A 14-item version of the Positive Affect and Negative Affect Schedule (PANAS) assessed how often people had felt six kinds of positive emotions (e.g., pleasant, happy, cheerful) and eight kinds of negative emotions (e.g., unpleasant, guilt, stress) in the past week (Kuppens & Diener, 2008). All 14 emotion items were assessed on a 7-point Likert scale ranging from 1 (*not at all*) to 7 (*all the time*), α = 0.85. Higher scores on each affect subscale represented greater experience of the respective emotion. The scale has

documented high reliability and validity in Chinese populations (Kong & Zhao, 2013). Although only PA was subject to analysis in the present study, both PA and NA items were presented to the subjects to prevent biases.

Brain imaging data acquisition

Whole-brain and MTL imaging data were collected via a Siemens 3T Prisma scanner with a 64-channel head coil at the Center for MRI Research of Tianjin Normal University. Subjects laid supine on the scanner bed and foam pads were used to minimize head motion. High-resolution T1-weighted structural images were extracted using MP-RAGE sequence with the following parameters: repetition time (TR) = 2,530 ms; echo time (TE) = 2.98 ms; multi-band factor = 2; flip angle = 7 degree; field-of-view (FOV) = 224 × 256 mm^2; slices = 192; voxel size = 0.5 × 0.5 × 1.0 mm^3. In addition, a high-resolution T2-weighted image was also acquired using a T2-SPACE sequence for use in MTL segmentation. The image plane was perpendicular to the main hippocampal axis and covered the whole MTL region via the following parameters: TR = 1,3150 ms; TE = 82 ms; filp angle = 150 degree; FOV = 220 × 220 mm^2; matrix = 512 × 512; thickness = 1.5 mm; slices = 60. Finally, the resting-state functional MRI images were further collected via the Gradient Echo type Echo Planar Imaging (GRE-EPI) sequences: TR = 2,000 ms; TE = 30 ms; multi-band factor = 2; flip angle = 90°; FOV = 224 × 224 mm^2; slice thickness = 2 mm; voxel size = 2 × 2 × 2 mm^3. The resting-state functional images included 300 volumes with a running time of 10 min 13 s. During the resting-state scanning, all subjects were required to relax and keep their eyes closed but to remain awake.

Structural MRI preprocessing

Structural MRI data were preprocessed using the Oxford Centre for Functional MRI of the Brain (FMRIB) Software Library voxel-based morphometry (FSL-VBM), a VBM style analysis toolbox implemented in FSL (version 6.0.0; part of the FSL package; http://www.fmrib.ox.ac.uk/fsl). Structural images of brains were extracted, tissue-type segmented, and then aligned to the grey matter template in the MNI152 standard space. The spatially normalized images were then averaged to create a study-specific template, at which the native grey matter images were then registered again using both linear and nonlinear algorithms. The registered partial volume images were then modulated by dividing them with the Jacobian of the warp field to correct for local expansion or contraction. The modulated segmented images, which represented GMV, were then smoothed with an isotropic Gaussian kernel with 3 mm standard deviation. The smoothed data were used for the traditional univariate analysis whereas the unsmoothed data were used for the MVPA.

Resting-state fMRI preprocessing

The resting-state fMRI data were firstly preprocessed via the wise-used GRETNA software and the AFNI toolbox. The scanner automatically discarded the first eight volumes in order to ensure the signal equilibrium. Furthermore, the first ten EPI volumes were also excluded for each subject to factor in the time needed to adapt to the scanner's environment and the issue of the magnetization disequilibrium.

The remaining 290 volumes were further slice-timing corrected, realigned, and registered to the standardized MNI space. Each fMRI volume was then segmented into different tissue types (i.e., gray matter, white matter, and cerebrospinal fluid) using DARTEL (Ashburner, 2007). We then performed temporal detrending, nuisance regression, and bandpass filtering using AFNI tools. Following a recent data analysis strategy (Lindquist et al., 2019), nuisance covariates, linear trends, and temporal filters (0.01~0.1 Hz) were entered in a single regression model to prevent the reintroduction of noise artifacts. In the current model, the nuisance covariates included the average signals from the cerebrospinal fluid and white matter, the global signal, and 24 motion parameters (Friston et al., 1996).

Segmentation of MTL sub-regions

MTL subfield volume was measured via the automatic segmentation of hippocampal subfields (ASHS) (Yushkevich et al., 2010, 2015). The ASHS approach separates hippocampal subfields based on a multi-atlas segmentation approach with joint label fusion that corrects for bias through machine learning. ASHS further utilizes the input of both high-resolution T1-weighted and T2-weighted images to obtain best separation. In doing so, the ASHS technique is automated at the MRI pre-processing, image separation, bias correction, and refining stages to parcellate the MTL into seven subregions, including CA1, CA2+3, the DG, the subiculum (SUB), the perirhinal cortex (PRC), and parahippocampus (PHC). Additional information about the ASHS technique and its differences from the manual segmentation of MTL may be found in Yushkevich et al. (2015) and software documentations made available at http://sites.google.com/site/hipposubfields/.

We used two approaches to adjust subfield volumes of the MTL to decrease individual variation in head size. First, we adjusted the hippocampal subfield volume in each hemisphere with an analysis of covariance-based formula:

$$\text{adjusted volume} = \text{raw volume} - b \times (\text{ICV} - \text{mean ICV})$$

In this formula, b represents the slope coefficient of the regression of ROI volume on ICV (Raz et al., 2005). We report all findings based on this adjustment approach. Secondly, all hippocampal subfields' volumes on each hemisphere were adjusted by the total hippocampus volume to validate our main findings. Several studies have demonstrated more advantages in compatibility with existing histopathologic knowledge compared to the FreeSurfer method (Sone et al., 2016).

Univariate and multivariate pattern analyses

First, we examined possible associations between PA and GMV in whole-brain level using a mixed-effects FLAME 1 model implemented in FSL. Specifically, this model incorporates both fixed effects (i.e., within-session across-time variances estimated in the first level analysis) and random effects (i.e., the true cross-session variance of first-level parameter estimates). The benefit of this approach is derived from its ability to model and estimate variances for different groups in the model, capturing potential associations between different variables. Here, maternal education, paternal education, age at MRI scan,

sex, and total GMV were included as covariates. In the regression analyses, covariates were entered into the first block of equations. In the second block, mean-centered PA scores were entered. Statistical results were determined at the cluster level ($z > 3.1$, $p < 0.001$) and at the family-wise error rate of 0.05 for the correction for multiple comparisons using Gaussian Random Field Theory.

Second, in MVPA, Epsilon-insensitive support vector regression (SVR) (Drucker et al., 1997) with a linear kernel, as implemented in PyMVPA (http://www.pymvpa.org) (Hanke et al., 2009), was employed to examine the possible associations between PA and GMV at the whole-brain level. A searchlight procedure with a three-voxel radius (Kriegeskorte et al., 2006) was used to assess the decoding accuracy in the neighborhood of each voxel. Based on prior studies (Lv et al., 2020; Q. Wang et al., 2021), we set the ε parameter in the SVR to be 0.01. A three-fold cross-validation analysis was conducted in the present study. The 321 subjects were divided into three groups of 107 subjects, with matched gender and PA scores. In each iteration, an SVR model was trained based on two groups of 214 subjects. It is worth noting that the training dataset was first standardized and then applied to the testing dataset. Once trained, this SVR model then was applied to test the generalization on the remaining group based on their brain imaging data. The voxel-wise accuracy of SVR prediction was then calculated as the Pearson's correlation coefficient between actual and predicted values of positive affect, and then transformed to the corresponding z-score maps. Finally, SVR predictions were thresholded using cluster detection statistics, with a height threshold of $z > 3.1$, and a cluster probability of $p < 0.05$, corrected for whole-brain multiple comparisons using Gaussian Random Field Theory.

Third, based on the hypothesis that the hippocampus is important for PA as well as the findings from the whole-brain analysis, we further examined the associations between MTL/hippocampal subfield volume and PA using linear regression. Parental education, sex, and age at MRI scan were included as covariates and the adjusted hippocampal subfield volume as the outcome variable. Bonferroni correction was used to adjust for multiple comparisons ($0.05/14 = 0.0036$).

Fourth, the right PRC's mean time course was further calculated for each participant and was correlated with the time courses of the whole brain to construct the right PRC's functional connectivity map. This map was then converted to a *z* value map using Fisher's *r*-to-*z* transformation and smoothed with a Gaussian kernel with a full width half maximum of 6 mm. The smoothed data were used for univariate analysis such as the case with the GMV-related analysis excluding total GMV. Statistical results were determined at the cluster level ($z > 2.3$, $p < 0.001$) and at the family-wise error rate of 0.05 for the correction for multiple comparisons using Gaussian Random Field Theory. Additionally, we likewise utilized the unsmoothed rsFC data for MVPA in a manner similar as the above-mentioned analysis in GMV except for the number of each group.

Results

Demographics

In the whole sample (n = 321), the PA scores ranged from 10 to 50 (M ± SD = 27.46 ± 7.83) with no observed sex differences ($t_{(319)}$ = -1.564, p = 0.119) or variation across age (r = -0.021, p = 0.706), maternal education (r = 0.035, p = 0.530), paternal education (r = -0.025, p = 0.661), or total GMV (r = 0.006, p = 0.916). In the subsample with T2-weighted image data (n = 209), the M ± SD of PA scores were 27.45 ± 7.86. Consistent with the whole sample analysis, PA scores were not significantly correlated with age (r = 0.054, p = 0.441), maternal education (r = 0.004, p = 0.954), or paternal education (r = -0.087, p = 0.209) within this group. Further, PA scores were normally distributed (Shapiro-Wilk Z = 0.184, p > 0.05), further confirming the suitability of the parameter estimation in the following statistical analyses.

Associations Between Gmv And Pa In The Whole-brain Level

The present study aimed to explore the potential associations between MTL morphological and functional connectivity characteristics and PA. First, we used the traditional univariate analysis approach to examine whether there are significant correlations between specific brain regions' GMVs and PA at the whole-brain level but found no statistical evidence of such an effect. Considering higher sensitivity of MVPA on distributed coding of information and detecting brain-behavior associations than univariate analysis (Jimura & Poldrack, 2012; Q. Wang et al., 2014), we further applied this approach to examine the associations between PA and brain morphological index. As expected, MVPA revealed that PA was associated with the GMVs in several brain regions, such as the right hippocampus (peak MNI = 28, -22, -10, Z = 3.71), left parahippocampus (MNI = -26, -20, -24, Z = 3.88), left amygdala (MNI = -34, -8, -16, Z = 4.83), right precentral gyrus (MNI = 36, -14, 44, Z = 4.52), left lateral occipital cortex (LOC; MNI = -26, -70, 24, Z = 4.31), left frontal pole (FP; MNI = -16, 70, 6, Z = 4.66), right ventromedial prefrontal cortex (VMPFC; MNI = 6, 44, -24, Z = 4.22), right inferior frontal gyrus (IFG; MNI = 44, 28, 4, Z = 4.08), right subcallosal cortex (MNI = 2, 12, -24, Z = 4.73), and right cerebellum (MNI = 6, -52, -14, Z = 5.56) (Fig. 1A & Table 1). In probing the direction of the associations between these ROIs' GMVs and PA, an additional correlational analysis revealed that PA was positively associated with the GMVs in the hippocampus, VMPFC, FP, and cerebellum. In contrast, the remaining ROIs showed negative associations between their GMVs and PA.

Table 1
Brain regions whose GMVs predicted PA in multivariate analysis

Brain regions	Cluster size (voxels)	MNI Coordinates			Z score
		X	Y	Z	
L amygdala	35	-34	-8	-16	4.83
R hippocampus	11	28	-22	-10	3.71
L parahippocampus	7	-26	-20	-24	3.88
L Frontal pole	123	-16	70	6	4.66
R VMPFC	122	6	44	-24	4.22
R Subcallosal cortex	92	2	12	-24	4.73
R IFG	78	44	28	4	4.08
R Precentral gyrus	150	36	-14	44	4.52
R Cerebellum	126	6	-52	-14	5.56
L LOC	131	-26	-70	24	4.31
Abbreviation:					
VMPFC, ventromedial prefrontal cortex; IFG, inferior frontal gyrus; LOC, lateral occipital cortex.					

To directly compare the univariate and MVPA results, z statistics of each voxel in these ROIs' areas were plotted. As shown in the Fig. 1B, all paired-sample T-test revealed that the z statistics of the MVPA were significantly larger than those of the univariate analysis (all $ts > 20.12$, $ps < 0.0001$), and strongly distributed on the upper diagonal line (i.e., larger z scores), suggesting that the effect size was higher for MVPA compared to univariate analysis.

Direct Link Between Mtl Subfields' Volumes And Pa

Based on the significant correlations between GMV in the right hippocampus/PHC and PA observed in the whole-brain analysis, we further examined which MTL subfield volume was associated with individual's variability in PA. First, automatic segmentation of the medial temporal lobe is shown in Fig. 2. The MTL subfield volumes are listed in Table 2. All paired sample t-tests on the left versus right comparisons of volumetric data are presented in Table 2. Significant differences in volumes between the left and the right hemispheres were found in the CA1, CA2 + 3, DG, ERC, PRC, and SUB.

Table 2
Comparison of left and right subfield volumes with paired samples t-test

	Left Mean	Right Mean	*t* value	*p* value
CA1 mm^3	780	810	-5.43***	1.59e-07
CA2 + 3 mm^3	329	315	4.07***	6.74e-05
DG mm^3	808	949	-28.21***	< 0.0001
ERC mm^3	572	719	-23.51***	< 0.0001
PHC mm^3	2780	2765	0.61	0.542
PRC mm^3	3178	2927	8.17***	2.91e-14
SUB mm^3	582	435	38.38***	< 0.0001

Abbreviation: CA1, Cornu ammonis 1; CA2 + 3, Cornu ammonis 2 and 3; DG, dentate gyrus; ERC, entorhinal cortex; PHC, parahippocampus; PRC, perirhinal cortex; SUB, subiculum. *** p < 0.001.

Second, correlational analysis showed a significantly positive correlation between PA and GMV in only the right PRC (r = 0.221, p = 0.001) (Fig. 3A). Furthermore, linear regression models further evidenced this positive association between the two variables even after controlling for several covariates (β = 16.315, p = 0.0011, R^2 = 0.073, Bonferroni correction p = 0.015). In line with this outcome, we observed a significant association between the right PRC and PA (r = 0.232, p = 0.0004) (Fig. 3B) in the second adjustment method via total hippocampal volumes. After controlling for covariates, this association remained significant (β = 0.0014, p = 0.00021, R^2 = 0.087, Bonferroni correction p = 0.003). However, we did not identify any other significant findings in the remaining MTL subfields' volumes (all ps > 0.065, uncorrected). Importantly, the similar patterns were replicated (all corrected ps < 0.034) in the functional dataset (n = 183) after excluding the subjects with large head motion.

Prc-seed-based Rsfc Could Predict Individual's Pa

Here, we further explored how the right PRC modulates PA via specific functional connectivity with other brain regions. First, traditional univariate analysis was used to examine the associations between PRC-seed-based rsFC and PA (n = 183). Results showed that PA was positively correlated with the right PRC-seed-based couplings with the left LOC (MNI = -34, -70, 16, Z = 4.07) and right PHG (MNI = 26, -24, -24, Z = 3.99), while negatively with the couplings with the left DLPFC (MNI = -40, 20, 8, Z = 4.18) and left FP (MNI = -28, 60, 26, Z = 3.93) (Fig. 4A & Table 3).

Table 3
Brain regions whose functional connectivity with right PRC seed predicted PA in univariate and multivariate analysis

Brain regions	Cluster size (voxels)	MNI Coordinates			Z score
		X	Y	Z	
Univariate analysis					
L parahippocampus (+)	972	26	-24	-24	3.99
L Lateral occipital cortex (+)	991	-34	-70	16	4.07
L DLPFC (-)	531	-40	20	8	4.18
L frontal pole (-)	422	-28	60	26	3.93
Multivariate analysis					
L IFG	324	-38	22	12	5.10
L frontal pole	201	-18	58	-14	4.90
R VMPFC	129	4	52	0	5.74
R frontal pole	146	22	46	-18	5.12
DMPFC	121	0	56	20	4.87
L DLFPC	141	-26	48	20	3.86
L lateral orbitofrontal cortex	210	-42	32	-6	6.22
L Superior parietal lobule	210	-24	-50	36	5.37
R Superior parietal lobule	127	38	-48	54	4.42
L parahippocampus	226	-14	-22	-22	5.28
R Occipital pole	187	12	-92	22	4.87
R Middle cingulate cortex	185	4	-6	46	4.99
L Occipital pole	138	-6	-92	10	4.32
L Lateral occipital cortex	291	-24	-88	18	4.49
R COC	121	44	-18	16	5.75
L Middle temporal gyrus	117	-60	-42	-6	4.78
L Posterior cingulate cortex	115	-8	-36	14	5.88
R Lateral occipital cortex	114	22	-64	52	4.26

Abbreviation: VMPFC, ventromedial prefrontal cortex; IFG, inferior frontal gyrus; DLPFC, dorsolateral prefrontal cortex; DMPFC, dorsomedial prefrontal cortex; COC, central opercular cortex.

Brain regions	Cluster size (voxels)	MNI Coordinates			Z score
		X	Y	Z	
R cerebellum	176	16	-58	-52	5.01

Abbreviation: VMPFC, ventromedial prefrontal cortex; IFG, inferior frontal gyrus; DLPFC, dorsolateral prefrontal cortex; DMPFC, dorsomedial prefrontal cortex; COC, central opercular cortex.

In contrast, MVPA revealed that the functional connectivity of the right PRC seed with the fronto-parietal-occipital system successfully predicted individual variability in PA. The fronto-parietal system predominantly included the left inferior frontal gyrus (IFG; MNI = -38, 22, 12, Z = 5.1), left DLPFC (MNI = -26, 48, 20, Z = 3.86), left lateral orbitofrontal cortex (lOFC; MNI = -42, 32, -6, Z = 6.22), left FP (MNI = -18, 58, -14, Z = 4.90), right FP (MNI = 22, 46, -18, Z = 5.12), right VMPFC (MNI = 4, 52, 0, Z = 5.74), DMPFC (MNI = 0, 56, 20, Z = 4.87), left SPL (MNI = -24, -50, 36, Z = 5.37), right SPL (MNI = 38, -48, 54, Z = 4.42) (Fig. 4B & Table 3). The occipital system mainly included the left LOC (MNI = -24, -88, 18, Z = 4.49), right occipital pole (OP; MNI = 12, -92, 22, Z = 4.87), left OP (MNI = -6, -92, 10, Z = 4.32), and right LOC (MNI = 22, -64, 52, Z = 4.26). In addition, similar prediction brain regions also included the right middle cingulate cortex (MCC; MNI = 4, -6, 46, Z = 4.99), left PHG (MNI = -14, -22, -22, Z = 5.28), left posterior cingulate cortex (PCC; MNI = -8, -36, 14, Z = 5.88), left middle temporal gyrus (MTG; MNI = -60, -42, -6, Z = 4.78), right central opercular cortex (COC; MNI = 44, -18, 16, Z = 5.75), and right cerebellum (MNI = 16, -58, -52, Z = 5.01).

Discussion

The present study explored the neuroanatomical and functional substrates of PA, with particular focus on MTL subfield volumes and its functional couplings with other brain regions using univariate and MVPA approaches in a relatively large sample. At the whole-brain level, MVPA results revealed that the GMVs in the prefrontal-limbic-occipital system were associated with individual variability in PA. At the subfield level, linear regression analysis further revealed a positive association between the MTL subfields' GMV, particularly for the right PRC, and PA. At the functional level, univariate and MVPA both predicted the right-PRC-based functional couplings with the fronto-parietal-occipital system on PA. This study provides an early investigation into the contributions of the MTL subfields' structural architecture and functional organization on PA to highlight the importance of MTL, particularly the PRC, on human PA trait.

Our multivariate analysis revealed that individuals with higher PA also exhibited larger hippocampal volume but smaller amygdala volume, supporting past findings on adolescents (Whittle, Lichter, et al., 2014; Whittle, Simmons, et al., 2014). The hippocampus and amygdala have been widely thought to play critical roles in emotional responses and affect experiences (Mackiewicz et al., 2006; Waraczynski, 2016). Specifically, the amygdala processes social signals of emotion, particularly negative emotions (i.e., fear), and consolidates emotional memory (Richardson et al., 2004). Damage to this region can lead to impairments in the processing of faces and other social signals (Dalgleish, 2004) in addition to altering the subjective experiences of positive and negative affect (Hsu et al., 2005). Past fMRI studies found that emotional blunting negatively correlates with neural activation in the amygdala during the processing of

PA (Rahm et al., 2015). In contrast, hippocampal volume has been directly linked with PA during adolescence (Whittle, Lichter, et al., 2014; Whittle, Simmons, et al., 2014). Even among animal studies, there has been a consistent link between the subjective experiences of positive emotion and hippocampal cell proliferation (Wöhr et al., 2009; Yamamuro et al., 2010). Considering the functional coupling between these two brain regions (Smith et al., 2006), it has been proposed that amygdala-related emotional responses and hippocampus-related emotional memory might support the formation of human PA trait.

Beyond the whole volume of the hippocampus, MTL subfields' volume, especially the PRC, was observed to explain individual PA variability in the current study. This remained consistent across two different adjustment methods. Indeed, the MTL is a complex region and exhibits functional and structural specificity for its distinct subfields (Alkadhi & Dao, 2019). The PRC, a critical sub-structure anatomically located at the boundary between the medial temporal lobe and the ventral visual pathway, represents both within (i.e., face-face) and between-domain associations (i.e., face-name), as well as contributing to declarative memory (i.e., episodic and semantic memory) via an interaction way with the hippocampus (Naya, 2016). Larger PRC volume may also hint at a stronger positive emotion/affect associative memory with daily events for easier recall of PA experiences from long-term memory, further promoting the formation and development of said PA experiences. Consistent with this morphological finding, resting-state functional connectivity analyses evidenced right PRC-visual pathway couplings, including LOC and OP brain regions, which could predict individual PA trait. Taken together, our study extends the contribution of MTL on PA into its subfield of the PRC, which further improves our understanding of the neural mechanisms of PA formation.

In the current study, the fronto-parietal system, with particular emphasis on the volume in the IFG/FP and functional couplings of PRC-seed with several prefrontal and parietal cortices (i.e., IFG/FP/DLPFC/SPL), have been found to support the formation of PA. Such brain regions were thought to predominantly exert top-down emotion regulation to change individual subjective affect experiences (Ochsner et al., 2012). Emotion regulation reflects modulation to ongoing emotional responses through an active involvement of regulatory processes regardless of behavioral or cognitive strategies, such as situation modification, attentional deployment, cognitive change, and response modulation strategies (Aldao et al., 2010). Considerable task-based functional imaging results have demonstrated that emotion regulation depends on the aforementioned brain regions and its potential down-modulation site locations on amygdala-centered hub region in order to increase PA and decrease negative emotional responses (Ochsner, 2003). Dysfunctional coupling between the control system (i.e., prefrontal cortices), affect system (i.e., amygdala), and memory system (i.e., PRC) has been proposed to explain atypical PA and NA experiences (Etkin et al., 2015). We likewise observed the contribution of the PRC-IFG/FP functional coupling on PA, which further provides the underlying functional modulation pathway subserving to PA. We also found that GMV in VMPFC was associated with PA. This region generally integrates affective valuations of specific stimuli made by the amygdala with inputs from other regions, including hippocampus-related memory system that provide affective information about prior encounters with the stimuli (Cunningham et al., 2011). Lesions in this region directly damage the PA and NA responses independent of context in both humans and animals (Beer et al., 2003; Elisabeth A. Murray et al., 2007). Moreover, the resting-state

functional connectivity analysis further demonstrated the functional coupling between this region and the right PRC that could predict PA, which provide a potential pathway supporting the formation of PA. Hence, the prefrontal cortices are not only critical to affect-regulation but also support the affect experiences and valuations of stimuli, which both determine the generation and formation of human affect trait via interaction with the amygdala-related emotion and PRC-related memory system.

Aside from the control and emotion systems, the volumes of visual processing systems, subserved by LOC, are likewise critical for inversely predicting PA. The LOC in humans is known as the “extrastriate visual cortex” and has been considered to be a critical region on visual object perception (Emberson et al., 2017; Grill-Spector et al., 2001). Importantly, this region is connected to face-processing core networks, including fusiform face area (FFA) and occipital face area (OFA) (Nagy et al., 2012), and plays a crucial role in face discrimination and expression processing by sending primary sensory signals (Pitcher et al., 2014; Rossion et al., 2001). Moreover, the intrinsic functional coupling between LOC and FFA has been demonstrated to predict individuals’ ability to discriminate the identity of face images with noise (Hermann et al., 2015). Abnormal LOC-FFA functional connectivity is associated with dysfunctional face processing, especially among those with autism spectrum disorder (Nickl-Jockschat et al., 2015). Past neuroimaging studies have implicated the engagement of LOC on representations of facial expressions (Grecucci et al., 2010; Greening et al., 2018). Taken together, the visual processing network, including LOC and OP, may provide primary face-related processing signals that are further integrated to generate subjective experiences of facial expression, thereby being vital for the formation of human PA.

Functional connectivity analyses further revealed that the PRC-occipital system coupling predicted individual variability in PA using both the univariate and MVPA approaches. Combined with GMV findings, the right PRC hub region receives input from the visual information processing system and further integrates its emotional and affective content to generate PA experience, thereby restoring the human long-term memory system. Several studies have demonstrated the importance of the visual processing system on emotional and facial expression information processing (Pessoa & Adolphs, 2011). Hence, the occipital system was thought to provide basic emotional/affective information for the PRC memory system that then projects to the high-level prefronto-parietal control network for further integration and modulation.

In the univariate voxel-wise analysis, we did not observe any significant associations between the brain structural morphological features and PA. In contrast, the MVPA approach detected potential brain-behavior associations based on distributed representational patterns on voxels’ GMVs, consistent with previous studies that highlighted higher sensitivity in MVPA (Q. Wang et al., 2016, 2021). To date, this method has been widely employed to investigate the neural mechanisms of higher-level cognitive processes and various behavioral indexes (Haxby et al., 2014; Norman et al., 2006; Q. Wang et al., 2014), which opens a new opportunity to directly decode and understand how the human brain works. In our study, direct comparison likewise demonstrated higher sensitivity for MVPA relative to traditional voxel-wise analysis in several brain areas, especially in the MTL region. Higher sensitivity provides implications for further exploring whether the MTL subfields’ volume can predict individual variability in PA. Thus,

using MVPA to capture the associations between brain morphology and behavior-related performances or index may be beneficial in uncovering the underlying neural substrates of PA.

There are several limitations to consider in current study. First, the examined sample was young, ranging from ages 17–26, limiting the generalizability of findings to a wider age bracket. Further research is necessary to investigate the longitudinal development effects across the lifespan. Second, previous studies also found that the reward system (i.e., ventral striatum) is critical for PA, which was not observed in our study. On the one hand, prior studies have typically focused on the functioning of reward system but not its structural morphological characteristics (Nikolova et al., 2012). Thus, further experimental designs to dissociate functional and structural associations with PA may be needed in future efforts. On the other hand, human PA may depend on the topological organization of the whole-brain but not separated brain regions (Qi et al., 2020), which provides a potential explanation for why we did not find associations with the reward system. Third, the hippocampal subfields, including CA1-3, DG, and SUB, were not found to correlate with individual PA scores, which imply the possibility that PA depends on the integral neural circuitry between them. Finally, although we found significant correlations between MTL subfields' volume and PA, especially for PRC, the specific functional mechanisms of PRC on PA and causal relationship are still unknown. Thus, additional experiments to explore its cognitive functions are needed.

In conclusion, the present study explored the morphological and functional substrates of PA, with particular focus on the MTL and its subfields' volume, using both the univariate and multivariate pattern approach. Our findings revealed the importance of the MTL and its subfields' hippocampus/PRC in their relation to PA. Moreover, the fronto-parietal and visual system morphological substrates and functional couplings with PRC also involve the formation of PA. These findings provide novel insights into the cognitive and neural mechanisms of human affect, especially from the perspective of MTL and its sub-structure morphology.

Declarations

Funding

This study was supported by the National Natural Science Foundation of China (32000786, 31800920), Humanities and Social Science Fund Project of the Ministry of Education (20YJC190018), and Natural Science Foundation of Tianjin City (20JCYBJC00920).

Disclosure of potential conflicts of interest

The authors declare that they have no conflict of interest.

Research involving Human Participants

Ethnical approval: "All procedures performed in studies involving human participants were in accordance with the ethical standards of the Institutional Review Board (IRB) of the Tianjin Normal University and

with the 1964 Helsinki declaration and its later amendments or comparable ethical standards. Informed consent was obtained from all participants included in the study.”

Informed consent

Informed consent was obtained from all individual participants included in the study.

Data and code availability

The data that support the findings of this study are available from the Functional MRI Center at Tianjin Normal University (TJNU). Data and code are available from the corresponding authors with the permission of the TJNU.

References

1. Admon R, Lubin G, Stern O, Rosenberg K, Sela L, Ben-Ami H, Hendler T (2009) Human vulnerability to stress depends on amygdala’s predisposition and hippocampal plasticity. Proc Natl Acad Sci USA 106(33):14120–14125. https://doi.org/10.1073/pnas.0903183106
2. Aldao A, Nolen-Hoeksema S, Schweizer S (2010) Emotion-regulation strategies across psychopathology: A meta-analytic review. Clin Psychol Rev 30(2):217–237. https://doi.org/10.1016/j.cpr.2009.11.004
3. Alkadhi KA, Dao AT (2019) Effect of Exercise and Aβ Protein Infusion on Long-Term Memory-Related Signaling Molecules in Hippocampal Areas. Mol Neurobiol 56(7):4980–4987. https://doi.org/10.1007/s12035-018-1425-x
4. Ashburner J (2007) A fast diffeomorphic image registration algorithm. NeuroImage 38(1):95–113. https://doi.org/10.1016/j.neuroimage.2007.07.007
5. Barense M, Bussey T, Lee A, Rogers T, Saksida L, Murray E, Hodges J, Graham K, 1MRC (2002) &. *Feature ambiguity influences performance on concurrent discriminations in patients with extensive damage to the medial temporal lobe CD CD CD Barcodes: Low familiarity Conclusions Bugs : Moderate familiarity Animals : High familiarity*. 2002
6. Beer JS, Heerey EA, Keltner D, Scabini D, Knight RT (2003) The Regulatory Function of Self-Conscious Emotion: Insights from Patients with Orbitofrontal Damage. J Personal Soc Psychol 85(4):594–604. https://doi.org/10.1037/0022-3514.85.4.594
7. Bonnici HM, Chadwick MJ, Maguire EA (2013) Representations of recent and remote autobiographical memories in hippocampal subfields. Hippocampus 23(10):849–854. https://doi.org/10.1002/hipo.22155
8. Brown MW, Aggleton JP (2001) Recognition memory: What are the roles of the perirhinal cortex and hippocampus? Nat Rev Neurosci 2(1):51–61. https://doi.org/10.1038/35049064
9. Cao B, Passos IC, Mwangi B, Tannous J, Wu M, Zunta-soares GB, Soares JC (2017) *Hippocampal sub fi eld volumes in mood disorders*. *May 2016*, 1–7. https://doi.org/10.1038/mp.2016.262

10. Choi J, Jeong B, Polcari A, Rohan ML, Teicher MH (2012) Reduced fractional anisotropy in the visual limbic pathway of young adults witnessing domestic violence in childhood. NeuroImage 59(2):1071–1079. https://doi.org/10.1016/j.neuroimage.2011.09.033
11. Clark LA, Watson D, Leeka J (1989) Diurnal variation in the Positive Affects. Motivation and Emotion 13(3):205–234. https://doi.org/10.1007/BF00995536
12. Cunningham WA, Johnsen IR, Waggoner AS (2011) Orbitofrontal cortex provides cross-modal valuation of self-generated stimuli. Soc Cognit Affect Neurosci 6(3):286–293. https://doi.org/10.1093/scan/nsq038
13. Dalgleish T (2004) *Cognitive Approaches to Posttraumatic Stress Disorder: The Evolution of Multirepresentational Theorizing*. *130*(2), 228–260. https://doi.org/10.1037/0033-2909.130.2.228
14. Diamond LM, Aspinwall LG (2003) Integrating Diverse Developmental Perspectives on Emotion Regulation 27(1):1–6
15. Drucker H, Burges CJC, Kaufman L, Smola A, Vapnik V (1997) Support Vector Regression Machines. Analisis Standar Pelayanan Minimal Pada Instalasi Rawat Jalan Di RSUD Kota Semarang 3:103–111
16. Emberson LL, Crosswhite SL, Richards JE, Aslin RN (2017) The lateral occipital cortex is selective for object shape, not texture/color, at six months. J Neurosci 37(13):3698–3703. https://doi.org/10.1523/JNEUROSCI.3300-16.2017
17. Epstein RA (2008) Parahippocampal and retrosplenial contributions to human spatial navigation. Trends Cogn Sci 12(10):388–396. https://doi.org/10.1016/j.tics.2008.07.004
18. Etkin A, Büchel C, Gross JJ (2015) The neural bases of emotion regulation. Nat Rev Neurosci 16(11):693–700. https://doi.org/10.1038/nrn4044
19. Fenton AA (2010) *Method for inducing a psychotic state in an animal and a high throughput assay method for identifying a candidate agent having anti-psychotic properties*
20. Frodl T, O'Keane V (2013) How does the brain deal with cumulative stress? A review with focus on developmental stress, HPA axis function and hippocampal structure in humans. In *Neurobiology of Disease* (Vol. 52, pp. 24–37). Elsevier B.V. https://doi.org/10.1016/j.nbd.2012.03.012
21. Gosselin N, Samson S, Adolphs R, Noulhiane M, Roy M, Hasboun D, Baulac M, Peretz I (2006) Emotional responses to unpleasant music correlates with damage to the parahippocampal cortex. Brain 129(10):2585–2592. https://doi.org/10.1093/brain/awl240
22. Grecucci A, Soto D, Rumiati RI, Humphreys GW, Rotshtein P (2010) The interrelations between verbal working memory and visual selection of emotional faces. J Cogn Neurosci 22(6):1189–1200. https://doi.org/10.1162/jocn.2009.21276
23. Greening SG, Mitchell DGV, Smith FW (2018) Spatially generalizable representations of facial expressions: Decoding across partial face samples. Cortex 101:31–43. https://doi.org/10.1016/j.cortex.2017.11.016
24. Grill-Spector K, Kourtzi Z, Kanwisher N (2001) The lateral occipital complex and its role in object recognition. Vision Res 41(10–11):1409–1422. https://doi.org/10.1016/S0042-6989(01)00073-6

25. Hanke M, Halchenko YO, Sederberg PB, Hanson SJ, Haxby JV, Pollmann S (2009) PyMVPA: A python toolbox for multivariate pattern analysis of fMRI data. Neuroinformatics 7(1):37–53. https://doi.org/10.1007/s12021-008-9041-y
26. Haxby JV, Connolly AC, Guntupalli JS (2014) Decoding neural representational spaces using multivariate pattern analysis. Annu Rev Neurosci 37:435–456. https://doi.org/10.1146/annurev-neuro-062012-170325
27. Headey B (1993) *Bruce headey, jonathan kelley and alex wearing*. 63–82
28. Heller AS, Shi TC, Ezie CEC, Reneau TR, Baez LM, Gibbons CJ, Hartley CA (2020) Association between real-world experiential diversity and positive affect relates to hippocampal–striatal functional connectivity. Nat Neurosci 23(7):800–804. https://doi.org/10.1038/s41593-020-0636-4
29. Hermann P, Bankó ÉM, Gál V, Vidnyánszky Z (2015) Neural basis of identity information extraction from noisy face images. J Neurosci 35(18):7165–7173. https://doi.org/10.1523/JNEUROSCI.3572-14.2015
30. Hsu M, Bhatt M, Adolphs R, Tranel D, Camerer CF (2005) Neural systems responding to degrees of uncertainty in human decision-making. Science 310(5754):1680–1683. https://doi.org/10.1126/science.1115327
31. Isen (1993) Positive affect and decision making. *Handbook of Emotions*
32. Isen AM, Daubman KA, Nowicki GP (1987) Posit Affect Facilitates Creative Problem Solving 52(6):1122–1131
33. Jimura K, Poldrack RA (2012) Neuropsychologia Analyses of regional-average activation and multivoxel pattern information tell complementary stories. Neuropsychologia 50(4):544–552. https://doi.org/10.1016/j.neuropsychologia.2011.11.007
34. Kong F, Zhao J (2013) Affective mediators of the relationship between trait emotional intelligence and life satisfaction in young adults. Pers Indiv Differ 54(2):197–201. https://doi.org/10.1016/j.paid.2012.08.028
35. Kriegeskorte N, Goebel R, Bandettini P (2006) Information-based functional brain mapping. Proc Natl Acad Sci USA 103(10):3863–3868. https://doi.org/10.1073/pnas.0600244103
36. Kuppens P, Diener E (2008) The Role of Positive and Negative Emotions in Life Satisfaction. Judgm Nations 95(1):66–75. https://doi.org/10.1037/0022-3514.95.1.66
37. Lindquist MA, Geuter S, Wager TD, Caffo BS (2019) Modular preprocessing pipelines can reintroduce artifacts into fMRI data. Hum Brain Mapp 40(8):2358–2376. https://doi.org/10.1002/hbm.24528
38. Lunkenheimer ES, Olson SL, Hollenstein T, Sameroff AJ, Winter C (2011) Dyadic flexibility and positive affect in parent-child coregulation and the development of child behavior problems. Dev Psychopathol 23(2):577–591. https://doi.org/10.1017/S095457941100006X
39. Lv J, Wang Y, Wang X, Chen W, Shao Y, Zhou J, Chen Q (2020) Brain function alterations in patients with diabetic nephropathy complicated by retinopathy under resting state conditions assessed by voxel-mirrored homotopic connectivity. Endocr Pract 26(3):291–298. https://doi.org/10.4158/ep-2019-0355

40. Lyubomirsky S, King L, Diener E (2005) *The Benefits of Frequent Positive Affect: Does Happiness Lead to Success ? 131*(6), 803–855. https://doi.org/10.1037/0033-2909.131.6.803
41. Ma Q, Rolls ET, Huang C-C, Cheng W, Feng J (2022) Extensive cortical functional connectivity of the human hippocampal memory system. Cortex 147:83–101. https://doi.org/https://doi.org/10.1016/j.cortex.2021.11.014
42. Mackiewicz KL, Sarinopoulos I, Cleven KL, Nitschke JB (2006) *The effect of anticipation and the specificity of sex differences for amygdala and hippocampus function in emotional memory*. *Track II*
43. Macoveanu J, Lie H, Vinberg M, Harmer C, Macdonald P, Moos G, Vedel L, Miskowiak W (2021) Affective episodes in recently diagnosed patients with bipolar disorder associated with altered working memory-related prefrontal cortex activity: A longitudinal fMRI study. J Affect Disord 295(September):647–656. https://doi.org/10.1016/j.jad.2021.08.110
44. Martinotti G, Hatzigiakoumis DS, Vita O, De, Clerici M, Petruccelli F, Giannantonio M, Di, Janiri L (2012) *Anhedonia and Reward System: Psychobiology, Evaluation, and Clinical Features*. *2012*(December), 697–713
45. Murray EA, Richmond BJ (2001) Role of perirhinal cortex in object perception, memory, and associations. Curr Opin Neurobiol 11(2):188–193. https://doi.org/10.1016/S0959-4388(00)00195-1
46. Murray EA, O'Doherty JP, Schoenbaum G (2007) What we know and do not know about the functions of the orbitofrontal cortex after 20 years of cross-species studies. J Neurosci 27(31):8166–8169. https://doi.org/10.1523/JNEUROSCI.1556-07.2007
47. Nagy K, Greenlee MW, Kovács G (2012) The lateral occipital cortex in the face perception network: An effective connectivity study. Front Psychol 3(MAY):1–12. https://doi.org/10.3389/fpsyg.2012.00141
48. Naya Y (2016) Declarative association in the perirhinal cortex. Neurosci Res 113:12–18. https://doi.org/10.1016/j.neures.2016.07.001
49. Nickl-Jockschat T, Janouschek H, Eickhoff SB, Eickhoff CR (2015) Lack of Meta-Analytic Evidence for an Impact of COMT Val158Met Genotype on Brain Activation during Working Memory Tasks. Biol Psychiatry 78(11):e43–e46. https://doi.org/10.1016/j.biopsych.2015.02.030
50. Nikolova YS, Bogdan R, Brigidi BD, Hariri AR (2012) Ventral striatum reactivity to reward and recent life stress interact to predict positive affect. Biol Psychiatry 72(2):157–163. https://doi.org/10.1016/j.biopsych.2012.03.014
51. Norman KA, Polyn SM, Detre GJ, Haxby JV (2006) Beyond mind-reading: multi-voxel pattern analysis of fMRI data. Trends Cogn Sci 10(9):424–430. https://doi.org/10.1016/j.tics.2006.07.005
52. Ochsner K (2003) Rethinking feelings: Using fMRI to study the neurocognitive mechanisms of emotion control. Clin Neuropsychologist 17(1):85
53. Ochsner, Silvers JA, Buhle, and J. T (2012) Functional imaging studies of emotion regulation: a synthetic review and evolving model of the cognitive control of emotion. Ann N Y Acad Sci 1251:E1–E24. https://doi.org/10.1111/j.1749-6632.2012.06751.x
54. Pellman BA, Kim JJ (2016) What Can Ethobehavioral Studies Tell Us about the Brain's Fear System? Trends Neurosci 39(6):420–431. https://doi.org/10.1016/j.tins.2016.04.001

55. Perkinsporras L, Wikman A, Bhattacharyya M, Strike P, Steptoe A (2008) Optimism and quality of life following acute coronary syndrome. *SPRINGER*
56. Pessoa L, Adolphs R (2011) Emotion and the brain: Multiple roads are better than one. Nat Rev Neurosci 12(7):425. https://doi.org/10.1038/nrn2920-c2
57. Pitcher D, Duchaine B, Walsh V (2014) Combined TMS and fMRI reveal dissociable cortical pathways for dynamic and static face perception. Curr Biol 24(17):2066–2070. https://doi.org/10.1016/j.cub.2014.07.060
58. Pressman SD, Cohen S (2005) Does positive affect influence health? Psychol Bull 131(6):925–971. https://doi.org/10.1037/0033-2909.131.6.925
59. Qi R, Luo Y, Zhang L, Weng Y, Surento W, Jahanshad N, Xu Q, Yin Y, Li L, Cao Z, Thompson PM, Lu GM (2020) Social support modulates the association between PTSD diagnosis and medial frontal volume in Chinese adults who lost their only child. *Neurobiology of Stress*, *13*(November 2019), 100227. https://doi.org/10.1016/j.ynstr.2020.100227
60. Rahm C, Liberg B, Reckless G, Ousdal O, Melle I, Oa A, Agartz I, Rahm C, Reckless G, Ousdal O, Melle I, Andreassen OA (2015) *Negative symptoms in schizophrenia show association with amygdala volumes and neural activation during affective processing*. 1:213–220. https://doi.org/10.1017/neu.2015.11
61. Raz N, Lindenberger U, Rodrigue KM, Kennedy KM, Head D, Williamson A, Dahle C, Gerstorf D, Acker JD (2005) Regional brain changes in aging healthy adults: General trends, individual differences and modifiers. Cereb Cortex 15(11):1676–1689. https://doi.org/10.1093/cercor/bhi044
62. Richardson MP, Strange BA, Dolan RJ (2004) *Encoding of emotional memories depends on amygdala and hippocampus and their interactions*. *7*(3), 278–285. https://doi.org/10.1038/nn1190
63. Rossion B, Schiltz C, Robaye L, Pirenne D, Crommelinck M (2001) How does the brain discriminate familiar and unfamiliar faces?: A PET study of face categorical perception. J Cogn Neurosci 13(7):1019–1034. https://doi.org/10.1162/089892901753165917
64. Rowe G, Hirsh JB, Anderson AK (2007) *Positive affect increases the breadth of attentional selection*. *39*
65. Russell JA, Carroll JM (1999) *The Phoenix of Bipolarity: Reply to Watson and Tellegen (1999)*. *125*(5), 611–617
66. Smith APR, Stephan KE, Rugg MD, Dolan RJ (2006) Task and content modulate amygdala-hippocampal connectivity in emotional retrieval. Neuron 49(4):631–638. https://doi.org/10.1016/j.neuron.2005.12.025
67. Sone D, Matsuda H, Ota M, Maikusa N, Kimura Y, Sumida K (2016) Epilepsy & Behavior Impaired cerebral blood fl ow networks in temporal lobe epilepsy with hippocampal sclerosis: A graph theoretical approach. Epilepsy Behav 62:239–245. https://doi.org/10.1016/j.yebeh.2016.07.016
68. Squire LR, Stark CEL, Clark RE (2004) The medial temporal lobe. Annu Rev Neurosci 27:279–306. https://doi.org/10.1146/annurev.neuro.27.070203.144130

69. Suzuki WA, Naya Y (2014) The perirhinal cortex. Annu Rev Neurosci 37:39–53. https://doi.org/10.1146/annurev-neuro-071013-014207
70. Taylor CT, Lyubomirsky S, Stein MB (2017) Upregulating the positive affect system in anxiety and depression: Outcomes of a positive activity intervention. Depress Anxiety 34(3):267–280. https://doi.org/10.1002/da.22593
71. van den Heuvel MP, Pol HEH (2010) P.3.023 Exploring the functional brain network: how efficient is our brain? Eur Neuropsychopharmacol 20(3):S81. https://doi.org/10.1016/s0924-977x(10)70095-x
72. Vos R, Wael D, Larivière S, Caldairou B, Hong S, Margulies DS, Jefferies E (2018) Anat microstructural determinants hippocampal subfield Funct connectome embedding 115(40):2–7. https://doi.org/10.1073/pnas.1803667115
73. Wang Q, Chen C, Cai Y, Li S, Zhao X, Zheng L, Zhang H, Liu J, Chen C, Xue G (2016) Dissociated neural substrates underlying impulsive choice and impulsive action. NeuroImage 134:540–549. https://doi.org/10.1016/j.neuroimage.2016.04.010
74. Wang Q, Luo S, Monterosso J, Zhang J, Fang X, Dong Q, Xue G (2014) Distributed value representation in the medial prefrontal cortex during intertemporal choices. J Neurosci 34(22):7522–7530. https://doi.org/10.1523/JNEUROSCI.0351-14.2014
75. Wang Q, Wang Y, Wang P, Peng M, Zhang M, Zhu Y, Wei S, Chen C, Chen X, Luo S (2021) Neural representations of the amount and the delay time of reward in intertemporal decision making. Hum Brain Mapp 42:3450–3469
76. Wang SF, Ritchey M, Libby LA, Ranganath C (2016) Functional connectivity based parcellation of the human medial temporal lobe. Neurobiol Learn Mem 134(January):123–134. https://doi.org/10.1016/j.nlm.2016.01.005
77. Waraczynski M (2016) Toward a systems-oriented approach to the role of the extended amygdala in adaptive responding. Neurosci Biobehav Rev. https://doi.org/10.1016/j.neubiorev.2016.05.015
78. Whittle S, Lichter R, Dennison M, Vijayakumar N, Schwartz O, Byrne ML, Simmons JG, Yücel M, Pantelis C, McGorry P, Alle NB (2014) Structural brain development and depression onset during adolescence: A prospective longitudinal study. Am J Psychiatry 171(5):564–571. https://doi.org/10.1176/appi.ajp.2013.13070920
79. Whittle S, Simmons JG, Dennison M, Vijayakumar N, Schwartz O, Yap MBH, Sheeber L, Allen NB (2014) Positive parenting predicts the development of adolescent brain structure: A longitudinal study. Dev Cogn Neurosci 8:7–17. https://doi.org/10.1016/j.dcn.2013.10.006
80. Winterburn JL, Pruessner JC, Schira MM, Lobaugh NJ, Voineskos AN, Chakravarty MM (2013) *NeuroImage A novel in vivo atlas of human hippocampal sub fi elds using high-resolution 3 T magnetic resonance imaging*. 74:254–265. https://doi.org/10.1016/j.neuroimage.2013.02.003
81. Wöhr M, Kehl M, Borta A, Schänzer A, Schwarting RKW, Höglinger GU (2009) New insights into the relationship of neurogenesis and affect: Tickling induces hippocampal cell proliferation in rats emitting appetitive 50-khz ultrasonic vocalizations. Neuroscience 163(4):1024–1030. https://doi.org/10.1016/j.neuroscience.2009.07.043

82. Yamamuro T, Senzaki K, Iwamoto S, Nakagawa Y, Hayashi T, Hori M, Sakamoto S, Murakami K, Shiga T, Urayama O (2010) Neurogenesis in the dentate gyrus of the rat hippocampus enhanced by tickling stimulation with positive emotion. Neurosci Res 68(4):285–289. https://doi.org/10.1016/j.neures.2010.09.001
83. Yang H, Yang S, Isen A (2015) M. (n.d.). *Positive affect improves working memory: Implications for controlled cognitive processing Positive affect improves working memory : Implications for controlled cognitive processing*. 37–41. https://doi.org/10.1080/02699931.2012.713325. *February*
84. Yushkevich PA, Avants BB, Das SR, Pluta J, Altinay M, Craige C (2010) Bias in estimation of hippocampal atrophy using deformation-based morphometry arises from asymmetric global normalization: An illustration in ADNI 3 T MRI data. NeuroImage 50(2):434–445. https://doi.org/10.1016/j.neuroimage.2009.12.007
85. Yushkevich PA, Pluta JB, Wang H, Xie L, Ding S, Gertje EC, Mancuso L, Kliot D, Das SR, Wolk DA (2015) *Automated Volumetry and Regional Thickness Analysis of Hippocampal Subfields and Medial Temporal Cortical Structures in Mild Cognitive Impairment*. *287*(August 2014), 258–287. https://doi.org/10.1002/hbm.22627
86. Zeineh MM, Engel SA, Thompson PM, Bookheimer SY (2003) Dynamics of the hippocampus during encoding and retrieval of face-name pairs. Science 299(5606):577–580. https://doi.org/10.1126/science.1077775
87. Zeineh, M. M., Engel, S. A., Thompson, P. M., & Bookheimer, S. Y. (2003). Dynamics of the hippocampus during encoding and retrieval of face-name pairs. *Science*, *299*(5606), 577–580. https://doi.org/10.1126/science.1077775

Figures

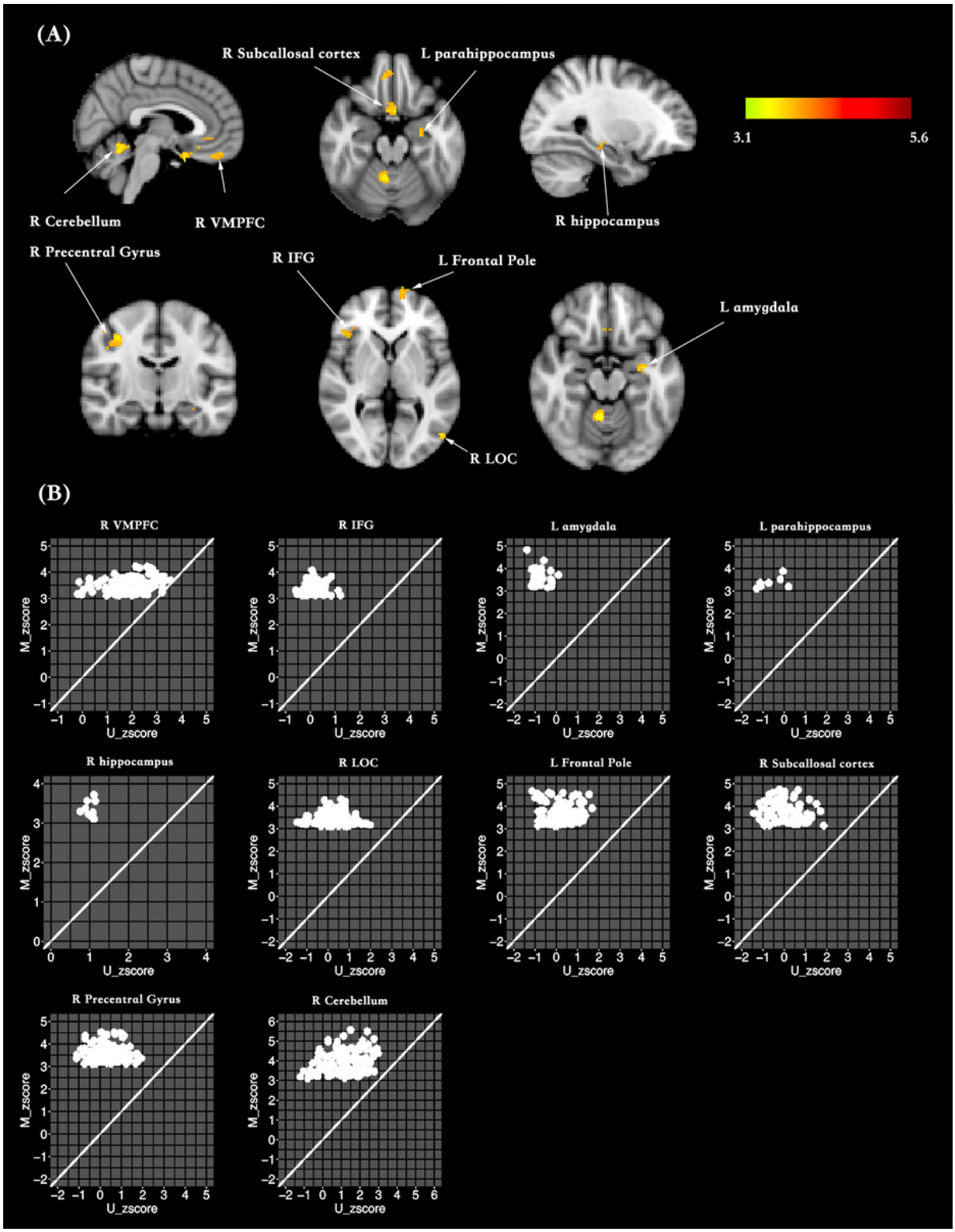

Figure 1

Grey matter volume's MVPA. A shows where the gray matter volume predicted individual's PA using MVPA. B displays the scatterplots of group-level z value of multivariate against univariate analysis for PA in the brain regions that significantly predict individual's PA.

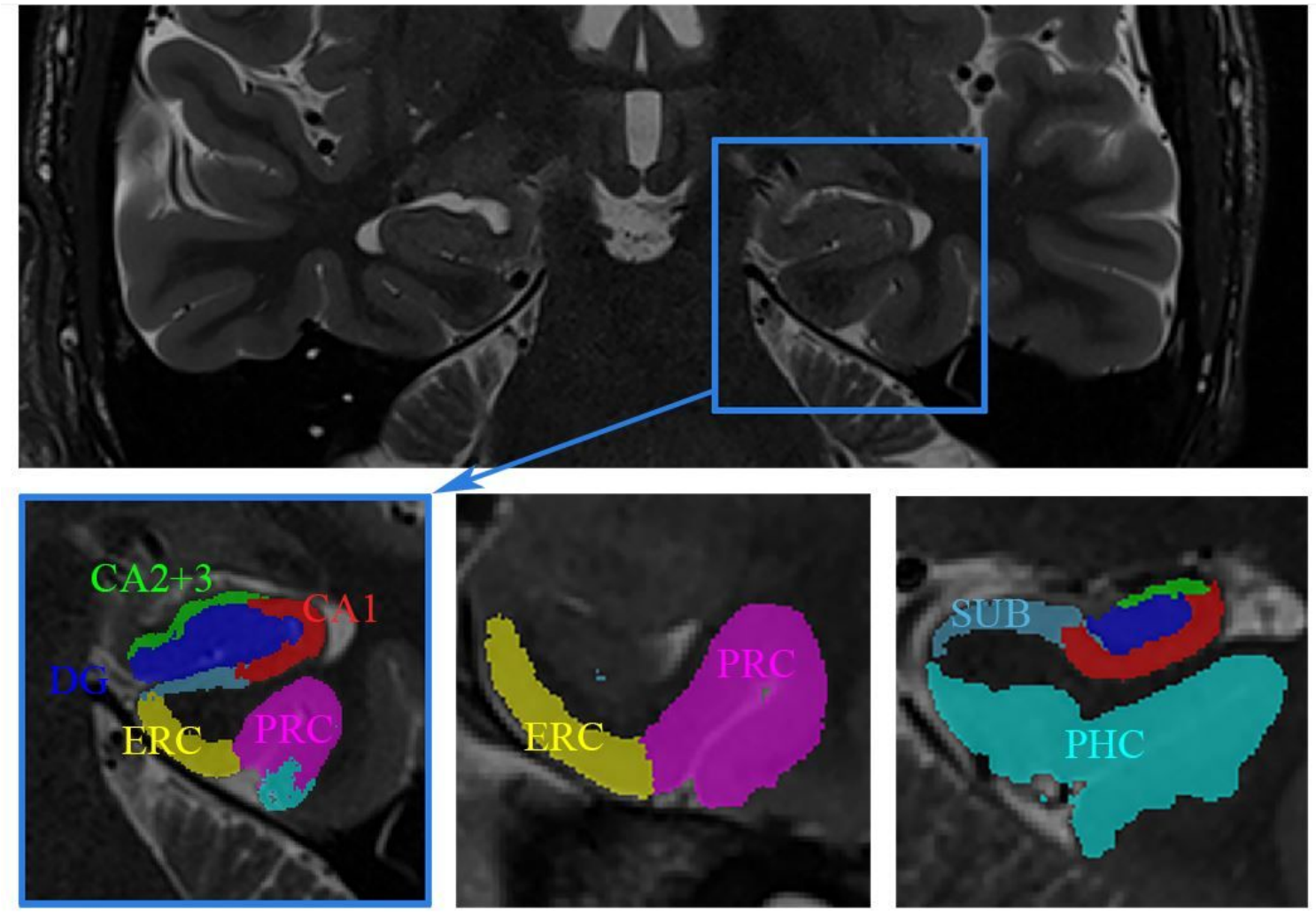

Figure 2

Visualization of the hippocampal subfield segmentations for a single subject and color key.

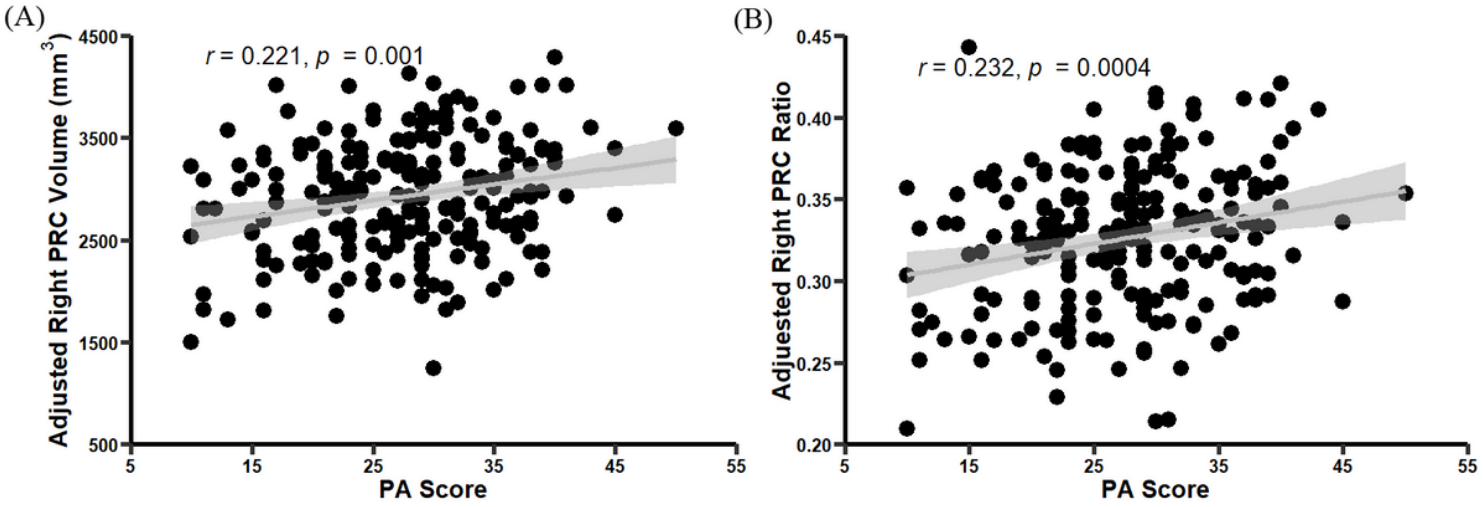

Figure 3

Scatter plots of linear correlation between the gray matter volume in PRC and PA via formula-based (A) and total hippocampus volume adjusted approaches (B).

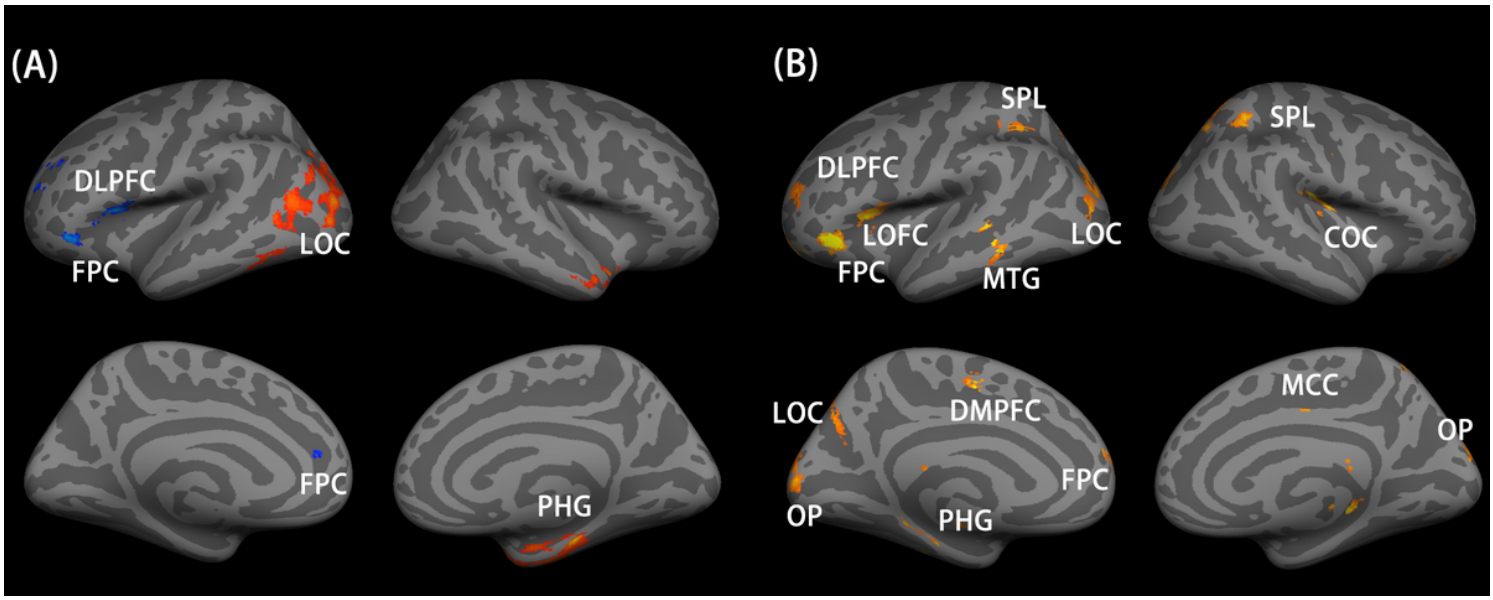

Figure 4

Right PRC-seed-based resting-state functional connectivity predicts individual's PA via univariate (A) and MVPA (B).